# Deep Learning-Based Autodetection of 5G NR mmWave Waveforms

Taekyun Lee\*, Abhinav Mahadevan<sup>†</sup>, Hyeji Kim\*, and Jeffrey G. Andrews\*, \*6G@UT, Dept. of ECE, The University of Texas at Austin, USA <sup>†</sup>Keysight Technologies, Santa Rosa, USA Email: taekyun@utexas.edu, abhinav.mahadevan@keysight.com, hyeji.kim@austin.utexas.edu, jandrews@ece.utexas.edu

Abstract—Wireless use cases such as spectrum sharing and Massive Machine Type Communications (mMTC) can benefit from the detection of unknown signals, which includes estimating their received power as well as other key characteristics such as bandwidth, modulation type, and waveform. While conventional signal detection methods are susceptible to noise, deep learning (DL) models offer a more robust alternative. Previously, DL models were used for solving simpler problems, focusing mainly on modulation recognition. We propose an advanced DL neural network structure that extracts the parameters of 5G NR frequency range 2 (FR2) mmWave test model waveforms. We evaluate our framework on a state-of-the-art signal generator and vector signal analyzer (VSA) that mimics real-world detection. Our work shows that incorporating curriculum training (CT) on both additive white Gaussian noise (AWGN) and frequency shift error enhances the model's accuracy across all SNR and frequency shift ranges. We further enhance the accuracy by employing the error vector magnitude (EVM) function to prioritize the top five scored parameters and validate selected parameters. As a result, our method consistently achieves an accuracy rate exceeding 90% when extracting the key parameters from 5G NR FR2 mmWave waveforms at diverse noise levels.

# I. Introduction

Automatic detection and labeling of waveforms can play a crucial role in the operation of modern wireless systems. For example, preemptive waveform parameter detection enables spectrum sharing, helping secondary users to minimize interference with primary users, thus ensuring coexistence and reliable services [1], [2]. This is particularly useful in satellite networks where spectrum sharing allows both types of users to use the same frequency, given that the primary users' quality standards are met [3]. While satellite-terrestrial non-orthogonal multiple access (NOMA) is a practical solution for secondary users with extremely low power [4], it traditionally necessitates cooperation between satellite and terrestrial terminals. However, identifying primary users' signals allows spectrum sharing to work even without coordination.

Similarly, Internet of Things (IoT) devices to connect, interact, and share data, Massive Machine Type Communications (mMTC) supports massive access with high interconnection

This work was partly supported by NSF Award CNS-2148141, as well as ARO Award W911NF2310062, ONR Award N00014-21-1-2379, NSF Award CNS-2008824, and Keysight Technologies through the 6G@UT center within the Wireless Networking and Communications Group (WNCG) at the University of Texas at Austin.

density, which assumes numerous low-power user equipments (UEs) [5]. For signal transmission, both the transmitter and receiver should know waveform parameters, such as carrier frequency, bandwidth, subcarrier spacing, and modulation. To achieve frame synchronization in both the transmitter and receiver, we can execute random initial access [6], especially from primarily inactive UEs. This process adds significant overhead to the system. However, preemptive signal parameter detection can facilitate communication via low-power devices without synchronization between the transmitter and receiver.

Previous works mainly focus on automatic modulation classification (AMC), detecting the modulation of single-carrier waveforms. One straightforward method for classifying the modulation of the waveforms is to capture specific features in each case and rigidly classify the waveforms [7], [8]. Another common approach employs a likelihood-based method, which is optimal in the Bayesian context [9], [10]. More recently, various deep learning (DL) frameworks like Convolutional neural networks (CNNs) [11], [12], and recurrent neural networks (RNNs) [13] have been applied to modulation recognition problems. An integrated model, the MCLDNN [14] and PET-CGDNN [15] has been developed to pursue better accuracy, representing the current state-of-the-art.

A further difficulty arises when applying the above frameworks to the 5G new radio (NR) millimeter wave (mmWave) waveforms specified in the 3rd generation partnership project (3GPP) technical specifications (TS) 38.211 [16], where we aim to recover various waveform parameters such as the bandwidth and modulation scheme in a noisy environment. Unlike single-carrier waveforms, the 5G NR mmWave waveform is OFDM with scalable numerology, so it comprises subcarriers of unknown width and modulation across multiple resource blocks (RBs).

In this work, we extend the techniques of automatic modulation recognition to identify multiple parameters. These include power allocation, bandwidth, subcarrier spacing, and the modulation scheme. We introduce a new DL structure that can accurately classify 5G NR mmWave waveforms, even in situations where there is scarce data for each label. The contributions of our proposed approach are as follows:

• Our method introduces a novel DL structure designed to extract unknown parameters from 5G NR mmWave signals

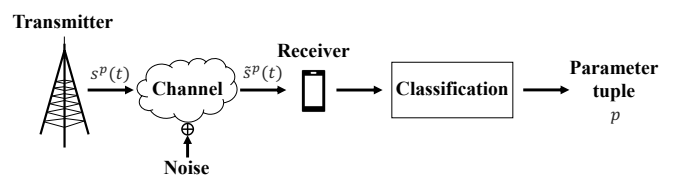


Fig. 1: Illustration of the proposed 5G NR mmWave transmission scenario.

for analysis.

- We incorporate and show the effectiveness of curriculum training (CT) to ensure adaptability across two distinct forms of degradation, namely additive white Gaussian noise (AWGN) and frequency shifts.
- We propose a Top-5 candidate trial algorithm. Beyond a basic DL model, we can make better estimates with assistance from vector signal analyzer (VSA) feedback.
- Our method demonstrates an enhanced accuracy rate of approximately 0.7, distinguishing itself from existing methods that are developed mainly for single-carrier waveforms.

#### II. PROBLEM STATEMENT

Generally, which parameters should we extract to effectively "detect" an unknown waveform? We decided on four parameters: the type of Test Model m, the bandwidth B, the subcarrier spacing configuration  $\mu$ , and the modulation scheme g. Here is our reasoning for selecting these four parameters.

Although an incorrect carrier frequency reference can lead to demodulation errors [17], we assume that our target carrier frequency is fixed at 28 GHz. Then, by removing the subcarrier spacing and determining the length of each RB, we can accurately delineate the structure of the resource grid. This calls for detecting B,  $\mu$ , and g. Also, by identifying specific standard waveforms m, we can know the contents of the waveform within each RB. Techniques such as parallelization and fast Fourier transform (FFT) can then be employed to identify its components [18]. As shown in Fig. 1, we consider a signal parameter detection problem for noise-added 5G NR mmWave signals. Detailed explanations of the above parameters are in Section IV-A.

The structure of the source signal s(t) with input parameters  $p = (m, B, \mu, g) \in \mathcal{P}$  is given by

$$s^{p}(t) = \sum_{k=0}^{N_{s}^{(B)}-1} c_{k}^{(m,\mu,g)} \cdot e^{j\left(2\pi k f\left(t - N_{CP}^{(\mu)} \cdot T_{c}\right)\right)}, \tag{1}$$

where subcarrier spacing defined as  $N_{\rm CP} = 15 \times 2^{\mu} ({\rm kHz})$  which is a function of  $\mu$ , and the number of subcarriers defined as  $N_s$ , which is a function of B. Carrier frequency f and the coherence time  $T_{\rm c}$  are constant values. Each element p in the ordered set P has a corresponding index, denoted by p = P[i].

Various types of noise can be added to s(t) which complicates the problem. We categorize the potential noise types in the received signal into two groups. The first is the additive white Gaussian noise  $\varepsilon_{AWGN}$ , which represents the ratio of the strength of the desired signal to background noise or

undesired signals. It can be disturbances such as intermodulation, thermal, and electronic disruptions in the transmission process. The second is a frequency shift error  $\varepsilon_{\Delta f}$ , which is the difference between the actual transmit frequency and the assigned frequency, stemming from issues like inadequate transmitter performance, receiver issues, baseband recovery problems, and flaws with reference clocks. Therefore, received signal  $\tilde{s}(t)$  is given by

$$\tilde{s}^{p}(t) = \sum_{k=0}^{N_{s}^{(B)}-1} \left( c_{k}^{(m,\mu,g)} + \varepsilon_{\text{AWGN}} + \varepsilon_{\Delta f} \right) \cdot e^{j\left(2\pi k f\left(t - N_{\text{CP}}^{(\mu)} \cdot T_{c}\right) + \phi\right)},$$
(2)

where  $\phi$  stands for a random phase offset value.

In this study, we focus on extracting the unidentified parameter tuple p from the signal  $\tilde{s}^p(t)$ . Our objective is to minimize the probability of error

$$P(\text{error}) = \frac{\sum_{p \in \mathcal{P}} \mathbb{I}(m(s^p) \neq p)}{|\mathcal{P}|},$$
 (3)

utilizing a function m that maps input  $\tilde{s}^p \in \{z \mid z(t) \in \mathbb{C}\}$  to output  $p \in \mathcal{P}$ . Given the numerous potential combinations in p, identifying the parameters of the waveform proves to be a challenging task.

#### III. THE PROPOSED APPROACH

Fig. 2 shows the steps of our proposed method. A signal is generated by a signal generator and sent to the VSA with unknown parameters. Inside the VSA, a DL classifier finds the parameter tuple p. Then the VSA verifies whether the parameter tuple p is correct.

#### A. Model structure of the proposed model, NRCLDNN

To solve  $\min_m P(\text{error})$ , function m is approximated using a DL model, denoted as M. The weights of M are optimized by minimizing the following problem

$$L^* = \min_{\mathbf{M}} \left( \mathbb{E}_{p \in \mathcal{P}} \left[ CE \left( \mathbf{M} \left( \tilde{s}^p \left[ n \right] \right), p \right) \right] \right), \tag{4}$$

where CE is the cross-entropy loss, and  $\tilde{s}^p[n]$  is the input discrete signal.

Fig. 3 provides an overview of our proposed DL architecture, new radio convolutional long short-term deep neural network (NRCLDNN). For the structure of the DL classifier, we adopt the MCLDNN framework introduced in [14]. This framework was initially designed for modulation recognition in single-carrier waveforms using I/Q data. Our approach differs structurally from previous works in that we changed I and Q data to magnitude and phase data, used only the

Fig. 2: Procedure flow for signal parameter detection and vector signal analyzer (VSA) configuration.

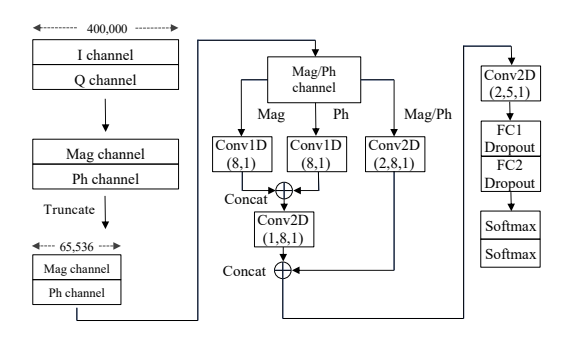


Fig. 3: The model architecture of NRCLDNN.

truncated amount of the signal, and set the filter size to 1, as described below.

First, we transform the input consisting of the I and Q values into the magnitude and phase values. This transformation is essential due to random signal rotations in the I/Q plane. By expressing the data in magnitude and phase terms, the magnitude remains unaffected by I/Q rotations while the phase undergoes a consistent shift. This representation enhances the resilience of the DL model to I/Q rotations. Second, we set the filter size in convolution layers to 1. When the filter size exceeds 1, the model becomes less generalizable and overfits the training data.

For maintaining uniform input dimensions, we retain only the first 65,536 symbols. The empirical analysis indicates that this length is optimal, providing ample representation without leading to a large input size.

The processed magnitude and phase signals then pass through three distinct pathways. Both the magnitude and phase signals pass through a 1D convolution layer. Simultaneously, a combined magnitude/phase signal passes through a 2D convolution layer, capturing the spatial correlations corresponding to the matching indices of magnitude and phase. These pathways are subsequently merged and further refined via two additional 2D convolution layers, enhancing the investigation of their spatial inter-relationships.

After extracting features from the previously described processes, the architecture incorporates two fully connected layers, each having a tangent hyperbolic (tanh) activation

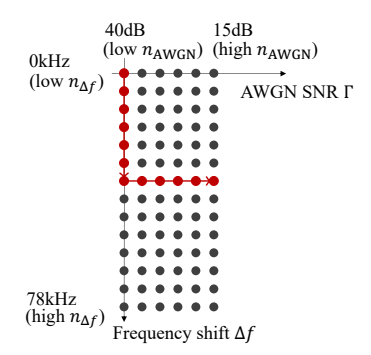


Fig. 4: Trajectory of  $\Gamma$ ,  $\Delta f$  in CT. The training starts with the frequency shift  $\Delta f = 0$  kHz frequency-shifted dataset. The value of  $\Delta f$  gradually increases to 36 kHz, then AWGN is added from SNR  $\Gamma = 40$  dB to 15 dB. It concludes with training set at low  $\Gamma$  and high  $\Delta f$  value.

function. A dropout rate of 0.5 is applied to minimize the risk of overfitting or underfitting the model. Subsequently, two softmax layers are introduced. The result is a probability vector for each label, which undergoes back-propagation and is compared to the target output, represented by a one-hot vector.

# B. Curriculum training

We modify two types of noise  $\varepsilon_{AWGN}$  and  $\varepsilon_{\Delta f}$  by adjusting the parameters: the AWGN signal-to-noise ratio (SNR)  $\Gamma$  and the frequency shift  $\Delta f$ , respectively. The AWGN SNR  $\Gamma$  is defined as

$$\Gamma = \frac{|s^p|^2}{\sigma_{\text{AWGN}}^2} \tag{5}$$

where  $\varepsilon_{\text{AWGN}} \sim \mathcal{N}(0, \sigma_{\text{AWGN}}^2)$ . While  $\Delta f$  is not represented in a closed form as (5),  $\varepsilon_{\Delta f}$  increases proportionally with  $\Delta f$ .

In our approach, we employ CT. Initially, the model is trained on coefficients derived from low-noise data. Subsequently, it is applied to high-noise data, enabling generalization across various noise levels. Our study covers  $\Gamma$  ranging from 15 dB to 40 dB and  $\Delta f$  ranging from 0 to 78 kHz.

As shown in Fig. 4, in our experiments, we detail the CT process of how we move through different noise levels. The

process begins at the point  $(\Gamma, \Delta f) = (40 \text{ dB}, 0 \text{ kHz})$  which has low  $\varepsilon_{\text{AWGN}}$  and low  $\varepsilon_{\Delta f}$ . We initially progress to points with maintaining  $\Gamma$ , gradually increasing  $\Delta f$  by 6 kHz until we reach  $(\Gamma, \Delta f) = (40 \text{ dB}, 36 \text{ kHz})$ , the point with higher  $\varepsilon_{\Delta f}$ . Subsequently, we decrease  $\Gamma$  by 5 dB until approaching the final point  $(\Gamma, \Delta f) = (15 \text{ dB}, 36 \text{ kHz})$ , which has higher  $\varepsilon_{\text{AWGN}}$  and higher  $\varepsilon_{\Delta f}$ .

We selected  $\Delta f=36$  kHz to prevent a significant drop in model performance. Training the model with  $\Delta f=78$  kHz adversely affected its capacity to classify signals with  $\Delta f=0$  kHz accurately. As a result, we chose a midpoint for  $\varepsilon_{\Delta f}$  that can handle both high and low noise levels. For the lowest  $\Gamma$  value, we chose 15 dB, because the VSA could not process signals with noise higher than 15 dB. To prevent overfitting and ensure effective adaptation to subsequent datasets, we limited our training to 15 epochs for each dataset rather than training until loss convergence. The result of limiting epochs can be observed in Fig. 5a.

#### C. Phase offset compensation through dataset amplification

Since the received signal, denoted as  $\tilde{s}(t)$ , undergoes an arbitrary phase shift  $\phi$ , each received signal experiences a rotation in the I/Q plane. Consequently, what the DL model **M** learns differs from the inference data, even if signals share the same parameter tuple p. To counter this challenge, we converted the I/Q channel to a magnitude/phase channel. The magnitude value remains stable despite phase shifts, and the phase value is moved by a constant when there is a phase shift. Dataset boosting is much simpler and more effective than teaching **M** an I/Q rotation from scratch.

Our strategy was to generate random phase-shifted data, amplifying the original dataset by a factor of r = 50 times. This prevented the model from overfitting to specific phase offsets and allowed for a better test dataset generalization.

# D. Top-5 candidate trial

When extracting parameters from the 5G NR mmWave signal, the error vector magnitude (EVM) measurement, which is fundamentally the root-mean-square (RMS) of the error vectors calculated with our waveform, can be used to verify the accuracy of the selected parameters. EVM measures the accuracy of symbol transmission within a constellation of a wireless signal. When we transmit bits with accurate waveform parameters, each bit aligns perfectly with its constellation points. However, any incorrect parameter can lead to misalignments, which can be captured by a high EVM value. The EVM value can be written as

$$EVM(\tilde{s}_i, p) = \sqrt{\frac{\sum_{i=1}^{N_s} \left(\tilde{s}_i - \tilde{s}_i^*(p)\right)^2}{N_s P_0}},$$
(6)

where  $N_s$  is the number of subcarriers,  $\tilde{s}_i$  is the i-th subcarrier of received signal, and  $\tilde{s}_i^*$  is the ideal denoised signal location of  $\tilde{s}_i$  in constellation. The constellation depends on the parameter tuple p. We need parameter information p to determine the ideal signal location.

For the received signal  $\tilde{s}_i$ , determining the corresponding parameter tuple p enables us to find the ideal location  $\tilde{s}_{i}^{*}$ for each point. If any estimated location deviates from the constellation point, the EVM will exceed the predefined threshold. Hence, we select the top-5 parameter candidates, setting K = 5, to verify the accuracy of our estimation by trying parameter tuple candidates one by one to input them into VSA for waveform interpretation. Starting with the parameter candidate of the highest probability, we store the parameter in the ordered set  $\mathcal{P}_{cand}$  and sequentially input it into the EVM function to check if it yields a reasonably low EVM value. If not, we try the next candidate to see if it yields the correct parameter tuple. The EVM threshold is set to 0.15 empirically. The technique is summarized in Algorithm 1. While this approach enables the model to consider a range of options, thereby enhancing its accuracy, it does come with the trade-off of increased processing time.

# **Algorithm 1** Top-*K* candidate trial

```
1: Input: signal \tilde{s}(t), DL model M, parameter tuple candi-
     date \mathcal{P}_{cand} = \emptyset
2: for k = 1, 2, ..., K do

3: I_k = \arg\max_{i=1, i \neq I_1, I_2, ..., I_{k-1}}^{|\mathcal{P}|} \mathbf{M}(\tilde{s}(t))[i]

4: \mathcal{P}_{cand} \leftarrow \mathcal{P}_{cand} \cup \mathcal{P}[I_k]
 5: end for
 6: Define the set of parameter tuple candidates and the EVM
     threshold.
 7: for k = 1, 2, ..., K do
         if EVM(\tilde{s}(t), \mathcal{P}_{cand}[I_k]) < threshold then
9:
              p_{\rm ans} = \mathcal{P}[I_k]
10:
              Break
         end if
11:
12: end for
13: Select the parameter tuple p_{ans}
```

#### IV. EXPERIMENT DETAILS

#### A. Dataset

First, we explain the four specific parameters we aim to detect.

Test Model (m). A Test Model denotes standard waveform configurations used for conformance testing. These standards evaluate metrics like base station RF output power, timing error, occupied bandwidth emissions, adjacent channel leakage ratio, and other unwanted emissions. Specific Test Models are tailored for distinct measurements outlined in 3GPP TS 38.141 [19]. TM (Test Model) 1.1 is primarily designed for examining various emissions and power parameters, predominantly utilizing QPSK modulation. TM 2 and 2a target power dynamics and frequency error at minimum power. Meanwhile, TM 3.1 and 3.1a concentrate on output power dynamics, signal quality, and error metrics at maximum power.

Bandwidth (B), subcarrier spacing ( $\mu$ ), modulation scheme (g). The bandwidth of the 5G NR mmWave is defined as the frequencies over which data can be transmitted. Subcarrier spacing refers to the frequency difference between

adjacent subcarriers in an OFDM system, ensuring they do not interfere with each other. The modulation scheme pertains to the technique used to encode data onto carrier waves.

Next, we describe how our dataset is set up based on the previous descriptions. To create the 5G NR mmWave test model dataset, we employed a signal generation software, Signal Studio, from Keysight Technologies. This work focuses on the frequency range 2 (FR2) range of the 5G NR frequency bands, which covers frequencies between 24.25 and 71.0 GHz, specifically focusing on 28 GHz. Our dataset contain m of TM1.1, TM2, TM2a, TM3.1, and TM3.1a. The modulation g of TM1.1 is set to QPSK, while g of TM2a and TM3.1a are set to 256QAM. However, TM2 and TM3 offer a range of g: QPSK, 16QAM, and 64QAM. Bandwidth B can be 50 MHz, 100 MHz, 200 MHz, and 400 MHz, which are independent of the test model and modulation, and the subcarrier spacing  $N_{\rm CP}$ can be either 120 kHz or 60 kHz. In total, these configurations yield 63 unique labels from different parameter combinations. Each label of the parameter tuple p corresponds to a specific waveform, making it crucial to identify all four parameters accurately. A misprediction in any of the four parameters will lead to an incorrect label assignment.

#### B. Experimental setup

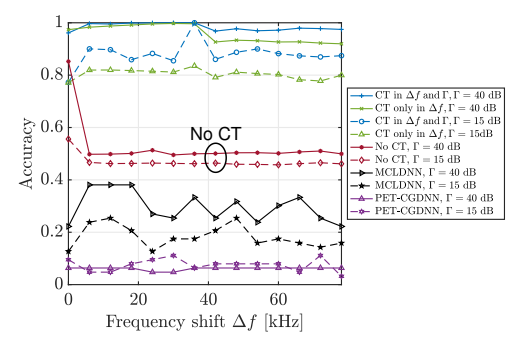
Our measurements were conducted using the Keysight VXG-C Signal Generator with the Keysight UXA Spectrum Analyzer. We selected a center frequency of 28 GHz for our tests due to its common usage in the 5G NR FR2 waveform frequency band. The analyzer was connected to the Keysight Pathwave Vector Signal Analysis software, which recorded the source waveforms successfully. The captured data was subsequently fed into the model for inference.

The experiment can be adapted to other experimental setups. The most challenging part is calculating the EVM value of the signal, but the calculation becomes straightforward with sufficient computational power at the receiver. We did not make restrictive assumptions about the parameters, allowing the method to be applied to different frequency signals and generic waveforms rather than limited to specific test models.

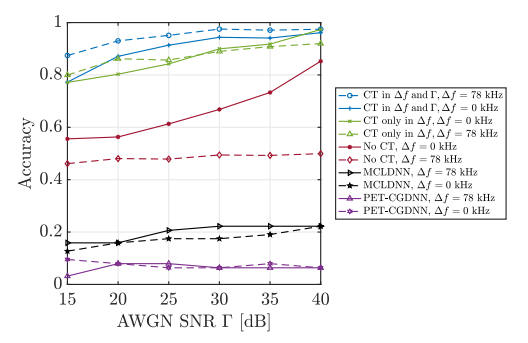
#### V. RESULTS AND DISCUSSIONS

In this section, we demonstrate the following: (i) our parameter detection model NRCLDNN outperforms the state-of-the-art DL models developed mainly for single-carrier waveforms; (ii) the curriculum training significantly improves the performance; and (iii) the top-*K* trial incorporating the EVM provides another significant gain in the parameter detection accuracy.

Comparison against existing approaches. To our knowledge, there are no existing traditional benchmarks that are directly comparable to our approach since this is the first work to detect waveform parameters from 5G NR mmWave waveforms. We evaluated our model against two state-of-the-art DL models, MCLDNN [14] and PET-CGDNN [15], which were initially developed for single-carrier waveforms. We trained our NR-CLDNN and the baselines MCLDNN and PET-CGDNN under



(a) Accuracy vs frequency shift, where the SNR of the AWGN noise  $\Gamma$  = 40 dB. 15 dB.



(b) Accuracy vs AWGN SNR, where the frequency shift  $\Delta f = 0$  kHz, 78 kHz.

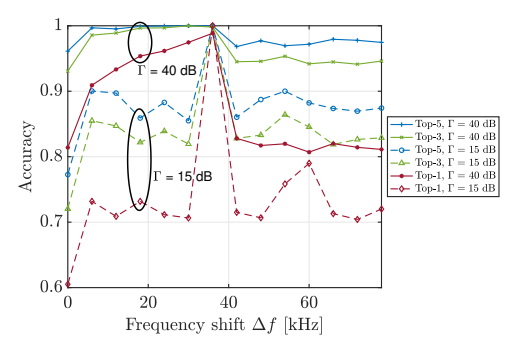
Fig. 5: Parameter detection accuracy with varying the types of noise added to the training datasets. Curriculum Training (CT) significantly improves the accuracy of parameter detection.

the same conditions for a fair comparison. As indicated in Fig. 5, the average accuracy of our NRCLDNN (without curriculum training (No CT)) surpasses that of MCLDNN by 24% and PET-CGDNN by 44%. The underperformance of the baseline models is perhaps due to their assumption that I/Q symbols lie on a specific configuration, which does not apply to 5G NR mmWave signals. With CT, we achieve even more gains as we describe next.

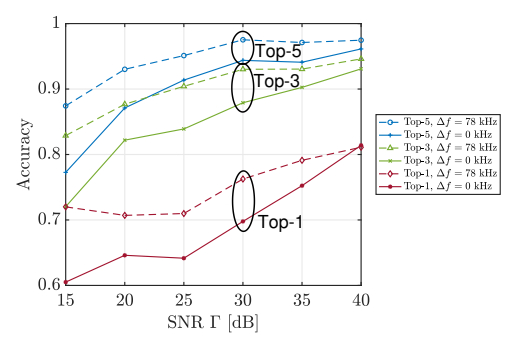
Effect of Curriculum Training (CT). Fig. 5 shows the performance comparison of our NRCLDNN in three training scenarios: CT applied to both  $\Gamma$  and  $\Delta f$ , CT applied only to  $\Delta f$ , and no CT. The model trained with CT on both  $\Gamma$  and  $\Delta f$  consistently outperforms the other methods in all noise ranges by a large margin, ranging from 20% to 50%, demonstrating the effectiveness of CT.

In Fig. 5a, when dataset's  $\Gamma$  is set at 40 dB, the model trained with CT on both  $\Gamma$  and  $\Delta f$  performs better, especially when  $\Delta f$  exceeds 36 kHz, compared to applying CT only to  $\Delta f$ . At a lower  $\Gamma$  of 15 dB, CT on both  $\Gamma$  and  $\Delta f$  becomes even more beneficial, consistently outperforming the strategy of CT for  $\Delta f$  alone. Fig. 5b demonstrates that applying CT on both  $\Gamma$  and  $\Delta f$  is generally more effective than CT only on  $\Delta f$ .

Effect of Top-K candidate trial. In Fig. 6, we plot the parameter detection accuracy of our NRCLDNN with top-1,3,



(a) Accuracy vs frequency shift, where the SNR of the AWGN noise  $\Gamma = 40$  dB. 15 dB.



(b) Accuracy vs AWGN SNR, where the frequency shift  $\Delta f = 0$  kHz, 78 kHz.

Fig. 6: Parameter detection accuracy with Top-K candidate trial. The top-5 candidate trial improves the detection accuracy by more than 20% compared to the Top-1 candidate trial.

and 5 trials as a function of the frequency shift (Fig. 6a) and the SNR of the AWGN noise (Fig. 6b) in the testing data. This result shows that increasing the number of trials from 1 to 3 achieves about 20% accuracy gain. We achieve even better accuracy by increasing the number of trials to 5, often close to accuracy  $\approx 1$  as shown in Fig. 6a.

In Fig. 6a, we also see that the accuracy of a Top-1 NRCLDNN is close to one when the frequency shift is 36 kHz and starts to drop as the frequency shift deviates from 36 kHz. This is because during the training of our NRCLDNN, we stopped at the frequency shift 36 kHz as depicted in Fig 4. Thus, when the testing frequency shift is close to 36 kHz, NRCLDNN with a single trial achieve accuracy  $\approx 1$  while the accuracy drops as the frequency shift departs from 36 kHz, as shown in Fig. 6a. Top-K trials successfully mitigate such performance degradation by incorporating the EVM feedback and exploring K possible parameters instead of only one.

Fig. 6b shows that there is consistently about a 20% difference in accuracy between selecting the top-5 choices compared to just the top-1 choice across a wide range of AWGN SNR values  $\Gamma$  from 15 to 40 dB. Here, we set the frequency shift to  $\Delta f$  as 0 kHz or 78 kHz – note that the training of the NRCLDNN was performed only for frequency shift training from 0 to 36 kHz. Our result implies that the top-5 candidate trial algorithm can enhance the accuracy even

# for frequency shift $\Delta f$ not covered in the training. VI. CONCLUSION

We proposed a novel approach for 5G NR mmWave test model waveform classification using DL and CT as the key tool. We achieve consistently high accuracy across various SNR and frequency shift levels by transforming the I/Q signal to magnitude/phase and applying a DL model combined with CT and top-5 candidate trials.

### REFERENCES

- S. Haykin, "Cognitive radio: Brain-empowered wireless communications," *IEEE J. Sel. Areas Commun.*, vol. 23, no. 2, pp. 201–220, Feb. 2005.
- [2] S. Srinivasa and S. Jafar, "Cognitive radios for dynamic spectrum access - the throughput potential of cognitive radio: a theoretical perspective," *IEEE Commun. Mag.*, vol. 45, no. 5, pp. 73–79, May 2007.
- [3] K. An, M. Lin, W.-P. Zhu, Y. Huang, and G. Zheng, "Outage performance of cognitive hybrid satellite-terrestrial networks with interference constraint," *IEEE Trans. Veh. Technol.*, vol. 65, no. 11, pp. 9397–9404, Nov. 2016.
- [4] X. Liu, K.-Y. Lam, F. Li, J. Zhao, L. Wang, and T. S. Durrani, "Spectrum sharing for 6G integrated satellite-terrestrial communication networks based on NOMA and CR," *IEEE Netw.*, vol. 35, no. 4, pp. 28–34, Jul./Aug. 2021.
- [5] X. Chen, D. W. K. Ng, W. Yu, E. G. Larsson, N. Al-Dhahir, and R. Schober, "Massive access for 5G and beyond," *IEEE J. Sel. Areas Commun.*, vol. 39, no. 3, pp. 615–637, Mar. 2021.
- [6] A. Omri, M. Shaqfeh, A. Ali, and H. Alnuweiri, "Synchronization procedure in 5G NR systems," *IEEE Access*, vol. 7, pp. 41286–41295, Mar. 2019.
- [7] A. Swami and B. M. Sadler, "Hierarchical digital modulation classification using cumulants," *IEEE Trans. Commun.*, vol. 48, no. 3, pp. 416–429, Mar. 2000.
- [8] S. Huang, Y. Yao, Z. Wei, Z. Feng, and P. Zhang, "Automatic modulation classification of overlapped sources using multiple cumulants," *IEEE Trans. Veh. Technol.*, vol. 66, no. 7, pp. 6089–6101, Jul. 2017.
- [9] B. F. Beidas and C. L. Weber, "Asynchronous classification of MFSK signals using the higher order correlation domain," *IEEE Trans. Commun.*, vol. 46, no. 4, pp. 480–493, Apr. 1998.
- [10] A. Ramezani-Kebrya, I.-M. Kim, D. I. Kim, F. Chan, and R. Inkol, "Likelihood-based modulation classification for multiple-antenna receiver," *IEEE Trans. Commun.*, vol. 61, no. 9, pp. 3816–3829, Aug. 2013.
- [11] T. J. O'Shea, J. Corgan, and T. C. Clancy, "Convolutional radio modulation recognition networks," in *Proc. Int. Conf. Eng. Appl. Neural Netw.*, 2016, pp. 213–226.
- [12] M. Kulin, T. Kazaz, I. Moerman, and E. De Poorter, "End-to-end learning from spectrum data: A deep learning approach for wireless signal identification in spectrum monitoring applications," *IEEE access*, vol. 6, pp. 18484–18501, Mar. 2018.
- [13] S. Rajendran, W. Meert, D. Giustiniano, V. Lenders, and S. Pollin, "Deep learning models for wireless signal classification with distributed lowcost spectrum sensors," *IEEE Trans. Cogn. Commun. Netw.*, vol. 4, no. 3, pp. 433–445, Sep. 2018.
- [14] J. Xu, C. Luo, G. Parr, and Y. Luo, "A spatiotemporal multi-channel learning framework for automatic modulation recognition," *IEEE Wireless Comm. Letters*, vol. 9, no. 10, pp. 1629–1632, Jun. 2020.
- less Comm. Letters, vol. 9, no. 10, pp. 1629–1632, Jun. 2020.
  [15] F. Zhang, C. Luo, J. Xu, and Y. Luo, "An efficient deep learning model for automatic modulation recognition based on parameter estimation and transformation," *IEEE Commun. Lett.*, vol. 23, no. 10, pp. 3287–3290, Oct 2021.
- [16] 5G; NR; Physical channels and modulation (Release 17), document 3GPP TS 38.211, Jul. 2023.
- [17] T. Pollet, M. Van Bladel, and M. Moeneclaey, "BER sensitivity of OFDM systems to carrier frequency offset and Wiener phase noise," *IEEE Trans. Commun.*, vol. 43, no. 2,3,4, pp. 191–193, Feb./Mar./Apr. 1905
- [18] N. E. Tunali, M. Wu, C. Dick, and C. Studer, "Linear large-scale MIMO data detection for 5G multi-carrier waveform candidates," in Proc. Asilomar Conf. Signals, Syst., Comput., Jun. 2015, pp. 1–5.
- [19] 5G; NR; Base Station (BS) conformance testing Part 1: Conducted conformance testing (Release 17), document 3GPP TS 38.141, Jul. 2023.